Liquid Crystals
Publication details, including instructions for authors and subscription information:
http://www.informaworld.com/smpp/title~content=t713926090

Optical microscopy, multinuclear NMR (^{2}H, ^{14}N and ^{35}Cl) and X-ray studies of dodecyl-and hexadecyl-trimethylammonium chloride/water mesophases

E. S. Blackmore[a]; G. J. T. Tiddy[ab]
[a] Unilever Research, Port Sunlight Laboratory, Merseyside, England [b] Department of Chemistry and Applied Chemistry, Salford University, Salford, England

To cite this Article Blackmore, E. S. and Tiddy, G. J. T.(1990) 'Optical microscopy, multinuclear NMR (^{2}H, ^{14}N and ^{35}Cl) and X-ray studies of dodecyl-and hexadecyl-trimethylammonium chloride/water mesophases', Liquid Crystals, 8: 1, 131 — 151
To link to this Article: DOI: 10.1080/02678299008047336
URL: http://dx.doi.org/10.1080/02678299008047336

LIQUID CRYSTALS, 1990, VOL. 8, NO. 1, 131–151

Optical microscopy, multinuclear NMR (^2H, ^{14}N and ^{35}Cl) and X-ray studies of dodecyl- and hexadecyl-trimethylammonium chloride/water mesophases

by E. S. BLACKMORE and G. J. T. TIDDY†

Unilever Research, Port Sunlight Laboratory, Quarry Road East, Bebington, Wirral, Merseyside L63 3JW, England

(*Received 26 September 1989; accepted 11 December 1989*)

The liquid crystal phases occurring with the cationic surfactants dodecyltrimethyl ammonium chloride (C_{12}TAC) and hexadecyltrimethyl ammonium chloride (C_{16}TAC) in water have been examined using differential scanning calorimetry, low-angle X-ray diffraction and, in particular, multinuclear magnetic resonance spectroscopy. The dependence of water (^2H_2O), chloride (^{35}Cl), and surfactant (^{14}N) quadrupole splittings (Δ) on composition in the hexagonal and lamellar phase has been determined. For C_{12}TAC, from the ^{14}N Δ values, the location and ordering of the NMe_3^+ was found to be almost independent of composition for the H_1 phase, whereas at the higher surfactant concentration within the L_α phase the order increased gradually. Within the H_1 phase the ^{35}Cl Δ values are highly sensitive to composition and temperature. This implies that the chloride ions reside between the head groups at the highest water concentrations and are squeezed out as temperature or surfactant concentration increases. Water ^2H Δ values show a maximum as a function of composition allowing an estimate of 4·3 bound water molecules per surfactant for the H_1 phase and < 2 bound for the L_α phase to be made. For C_{16}TAC X-ray diffraction data shows that the gel phase occurring below 40°C has an interdigited monolayer structure. At temperatures above the gel phase, H_1 and L_α phases occur, these being separated by V_1 or intermediate phases. Broadly, similar NMR quadrupole splittings to those found for C_{12}TAC were measured for the H_1 and L_α phases of C_{16}TAC. Only ^2H Δ measurements could be made on the gel phase. The values are generally larger than those for the L_α phase, indicating an increase in water ordering because of the increased order of the surfactant layer.

1. Introduction

While the mesophase formation of monoalkyl anionic surfactants has been widely studied (for reviews see [1–4]) cationic surfactants have received far less attention. Recently we have reported a survey of liquid crystal formation of cationic surfactants [5], including both a review of the literature and experimental studies of *c.* 50 additional surfactants. These demonstrated that cationic surfactant behaviour strongly resembles that of anionic surfactants, with hexagonal (H_1) and lamellar (L_α) phases being commonly observed. Additionally, for short alkyl chain surfactants the compositions between H_1 and L_α have a bi-continuous cubic structure (V_1) while long chain surfactants form intermediate (*Int.*) phases in the region. The transition between the two types of behaviour occurs at somewhat larger alkyl chain size (C_{14}–C_{16}) for

† Also at Department of Chemistry and Applied Chemistry, Salford University, Salford M5 4WT, England.

0267–8292/90 $3.00

the cationic surfactants studied than for anionic surfactants such as soaps and alkyl sulphates (C_8–C_{12}). In addition, for hexadecyltrimethyl ammonium chloride (C_{16}TAC) we observed that the $H_1/Int./L_\alpha$ sequence was transformed to $H_1/V_1/L_\alpha$ on increasing temperatures [5]. Following this we have observed birefringent intermediate phases in long chain nonionic and zwitterionic surfactant systems [6, 7]. Thus, it appears that a general pattern of mesophase behaviour for all hydrocarbon surfactants which form H_1 and L_α is the sequence $H_1/V_1/L_\alpha$ for short chain derivatives changing to $H_1/Int./L_\alpha$ on increasing chain length. Since increasing temperature also causes this change in phase sequence we have suggested that alterations to alkyl chain flexibility with either chain length or temperature could be the origin of the behaviour. This is strongly supported by an examination of the H_1/L_α transition for fluorocarbon surfactants (much less flexible chains) where only *Int.* phases are observed [6, 8].

The exact structures, indeed, the number of phases occurring in the intermediate region are still not fully elucidated; for anionic surfactants there could be up to four different phases present [9, 10]. Most of the structures proposed involve various ordered long rod phases, where the rods are arranged in distorted hexagonal or rectangular lattices. These differ fundamentally from the usual mesophases in being biaxial [9–13] rather than uniaxial. Previously we have emphasized the close relationship between one of the intermediate phases and the L_α phases [6, 8, 13]. This has been shown to consist of a layer structure where the layers comprise a tetragonal array of rods joined by fours [8, 10, 14]. A related phase structure consisting of layers formed by rods jointed by threes in a hexagonal array has been proposed by Luzzati *et al.* [15]. Thus these layer structures (lamellar phases with holes in the bilayers [16]–all uniaxial to date) form a set of intermediate phases distinct from the rod phases. Furthermore, non-cubic three dimensional network structures similar to the V_1 phase have been described theoretically [17] and do appear to occur [7] (see following paper [18]). Thus the intermediate phases may consist of three distinct classes where the aggregates are one dimensional, two dimensional or three dimensional, followed by further sub-division within each class according to the individual aggregate structure.

In this and a subsequent report [18] we describe a detailed investigation of the liquid crystal structures occurring in two cationic surfactant systems using mainly optical (polarizing) microscopy and multinuclear magnetic resonance spectroscopy, with some additional measurements by low-angle X-ray diffraction. The first system studied, dodecyltrimethylammonium chloride (C_{12}TAC)/water, has a known phase behaviour, the phase diagram and some X-ray data having been published by Broome *et al.* [19] and Balmbra *et al.* [20]. This surfactant was chosen so that the variation of the nuclear magnetic resonance parameters with composition for the known hexagonal and lamellar phases could be determined. Then these parameters can be employed to test structural models for intermediate phases of related surfactants [2], as well as giving information on headgroup/water and headgroup/counterion interactions. The second surfactant hexadecyltrimethylammonium chloride (C_{16}TAC) was selected because it exhibits both V_1, and *Int.* phases, giving perhaps the opportunity of studying the *Int.*–V_1 transition as well as allowing the *Int.* phase structures to be examined. Moreover, we can also see if the H_1 and L_α phases have different pretransitional behaviour according to whether V_1 or *Int.* phases occur.

We have employed a variety of techniques in the study. This first report describes the behaviour of water (^2H_2O), chloride (^{35}Cl) and surfactant (^{14}N) NMR quadrupole splittings (Δ) in the hexagonal and lamellar phase of C_{16}TAC and C_{12}TAC. In

addition, low angle X-ray and NMR, data are reported for the interdigited gel phase which is known to occur with C_{16}TAC [5]. These phase assignments are fully supported by observations made using optical microscopy and differential scanning calorimetry. In the second report we concentrate on the intermedite phases, using optical microscopy, NMR and low-angle X-ray diffraction to elucidate the number and structure of the phases [18].

2. Experimental

2.1. *Materials and sample preparation*

The surfactants were obtained from Eastmann Kodak as in the previous study [5]. They were recrystallized from acetone or acetone/isopropanol mixtures, vacuum dried and stored in a dessicator. Heavy water (^2H_2O) from BDH Ltd. (> 99·7 per cent) was used as supplied. Bulk samples were prepared by mixing the weighed constituents in tightly stoppered or glass-sealed tubes. After mixing (by heating and centrifugation) the contents were sealed in the appropriate NMR, tubes. The other physical measurements (DSC, low-angle X-ray diffraction, optical microscopy) (were made on the samples at the time of filling the NMR, tubes, and/or after the NMR, measurements were completed. This was done to ensure that no variation in composition occurred in samples employed for different techniques.

2.2. *Techniques*

Optical microscopy was carried out using a Reichert Thermopan microscope together with camera attachment and a Koffler hot-stage. The temperature were measured either using the mercury thermometer supplied with the hot-stage (± 1°) or with a Comark digital thermometer (± 0·5°).

The early NMR measurements were made using a Bruker Bkr 322-S pulsed spectrometer and variable temperature probe, operating at 8·0 MHz for ^{35}Cl resonance and 12·0 MHz for ^2H resonance. The $\pi/2$ pulse length was *c.* 15 μs for ^{35}Cl resonance and *c.* 10 μs for ^2H resonance. Quadrupole splittings were obtained from the free induction decay following a $\pi/2$ pulse, together with signal averaging and correction for the gaussian line shape where necessary as for previous work [21]. Temperatures were measured by inserting a thermometer into the probe before and after each measurement and were constant to within ± 1°C. Later NMR measurements were carried out using a Brucker CXP-300 spectrometer and variable temperature probe (± 1°) operating at frequencies of 21·68 MHz, 29·408 MHz and 46·07 MHz for ^{14}N, ^{35}Cl and ^2H resonances, respectively. The free induction decay following pulses of less than 10 μs was Fourier transformed to allow direct measurement of the quadrupole splitting from the spectra. Typically, 1000–10 000 scans were averaged for ^{14}N and ^{35}Cl spectra, with pulse rates of 20 s^{-1}; for ^2H spectra 50–100 scans were averaged at a rate of 2 s^{-1}. Where samples were measured on both spectrometers at a given temperature, the results were usually well within experimental error (± 3 per cent).

The low-angle X-ray scattering data were obtained using a Kratky camera with proportional-counter detection operated in continuous scan mode. Spectra were not corrected for slit-smearing effects as these were estimated to have little effect on the *d* spacings in this work. Samples were mounted either in 1 mm glass capillaries or sandwiched between pieces of mylar film to about the same thickness. High temperature work utilised the Anton-Paar Kratky variable temperature cell which is

continuously adjustable up to *c.* 70°C, to a precision of *c.* 0·5°C. All high-angle diffraction work was performed on a Phillips vertical diffractometer also using a continuous scan mode.

For DSC the samples (typically 3–6 mg) were sealed in aluminium pans. The measurements were made using a Perkin Elmer DSC Mk II at scanning rates of 5 or 10 K min^{-1} with a purge gas of nitrogen. The calorimeter had been calibrated for ΔH and temperature with indium and gallium samples at a scan rate of 10 K min^{-1}.

3. Results and discussion

3.1. *Dodecyltrimethylammonium chloride ($C_{12}TAC$)/water system*

3.1.1. *Optical microscopy and DSC measurements*

The phase diagram of C_{12}TAC taken from the work of Balmbra *et al.* [20] is shown in figure 1. The phases formed are micellar solution (L_1), globular (rod) micelle cubic phase (I_1); hexagonal phase (H_1); bicontinuous cubic phase (V_1) and lamellar phase (L_α). The lamellar phase only occurs above *c.* 27°C at equilibrium, but samples cooled to a few degrees below this temperature remain in the L_α structure for several hours. The H_1 and L_α phases in this system have the usual known structures, while the V_1 phase is a three dimensional network structure [1–4, 13]. Very recently [22, 23] it has been shown that the I_1 phase consists of short rod micelles arranged on the same cubic lattice (Pm3n) as that found in solid oxygen (γ-O_2) and fluorine (β-F_2) at 30 K and atmospheric pressure, or by nitrogen (N_2) at room temperature and 49 kbar. These rods have an axial ratio of *c.* 2 : 1 or smaller, and so they are very close to spherical shapes. The structures of bulk samples prepared for further measurements were first checked by polarizing microscopy. In every case the textures observed were

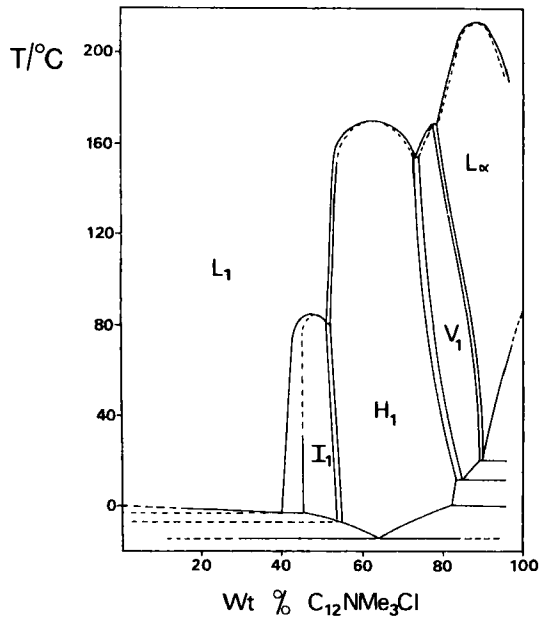

Figure 1. Phase diagram of dodecyltrimethylammonium chloride (C_{12}TAC)/water system. (Reprinted by permission from Balmbra, R. R., Clunie, J., and Goodman, J. F., 1969, *Nature, Lond.*, **22**, 159). L_1, micellar solution; I_1, globular micelle cubic phase; H_1, hexagonal phase, V_1, bicontinuous cubic phase, L_α lamellar phase. Copyright © 1969 Macmillan Magazines Ltd.

characteristic for the phase expected from figure 1. Thus, the very viscous cubic phase gave no birefringence, while lamellar and hexagonal phases gave mosaic/oily streaks textures [24] and non-geometric textures [24], respectively.

The DSC measurements gave no large transitions other than those associated with dissolution of the solid surfactant to form mesophases. Samples were first heated from 0–80°C, then cooled to −40°C followed by a second heating to 80°C. The anhydrous surfactant exhibited a very broad transition over *c.* 40–80°C (ΔH = 24·9 kJ mole^{-1}). This presumably arises from partial melting of the crystalline surfactant. The width of this transition may arise in part from the presence of a little water in the solid, since the carefully dried solids is reported to have a transition at 85°C (ΔH = 29·6 kJ mole^{-1}) [25] to form a soft solid or anhydrous mesophase. Polymorphism in anhydrous surfactants is commonplace [4], and so this was not pursued further. On addition of water to the surfactant this peak became indistinct. Only small, non-reproducible peaks (< 0·5 kJ mole^{-1}) were observed for samples not cooled below 0°C. These are probably due to dissolution of crystalline surfactant formed below the Krafft boundary. Samples cooled below 0°C gave larger transitions at *c.* −20°C to −30°C, assigned to ice/crystalline surfactant formation. They reappeared in the heating scans over the range −15°C to 10°C, according to composition. No evidence for gel formation as occurs with C_{16}TAC (see later) was obtained.

3.1.2. *NMR measurements*

Spectra representative of hexagonal and lamellar samples for C_{16}TAC are shown in figure 2; those of the C_{12}TAC samples were similar. The multiple peaks arise from the presence of an electric quadrupole moment in the nuclei studied. Both hexagonal phase and lamellar phase samples gave spectra typical of uniaxial mesophases (a powder doublet pattern for ^{2}H and ^{14}N (spin I = 1) and a powder triplet for ^{35}Cl (I = 3/2)) [26, 27]. The separation between the peaks is the quadrupole splitting (Δ). There is an extensive literature on the relation between Δ values and ion/molecular order in lyotropic mesophases [12, 21, 23, 26, 27] hence only a brief summary is given here.

We commence with a consideration of the ^{14}N data for C_{12}TAC (see figure 3). The Δ values increase only slightly with surfactant concentration across the H_1 region, are zero for the V_1 phase, and show an abrupt increase at the L_α transiton followed by a fairly sharp increase with concentration in the L_α phase. The data are in excellent agreement with a previous report [28] of ^{14}N values for a single C_{12}TAC composition (63·3 per cent in ^2H_2O) over the temperature range 20–80°C, including the slight decrease on increasing temperature in the H_1 phase.

For uniaxial mesophases the quadrupole splitting is a function of an order parameter (S) and the quadrupole coupling constant (χ) [26],

$$\Delta = \tfrac{3}{4}\chi S. \qquad (1)$$

The latter (χ) is determined by the magnitude and direction of electric field gradients at the ^{14}N nucleus. In the absence of molecular motions, it is not immediately obvious which are the three principal axes to describe the field gradient axes, except that we expect the major axis to lie fairly close to the N–CH_2 bond. However, since the attached alkyl chain up to a C_5 length does influence the value of χ [29], we cannot be certain that it is exactly along this bond [23]. An additional uncertainty arises with

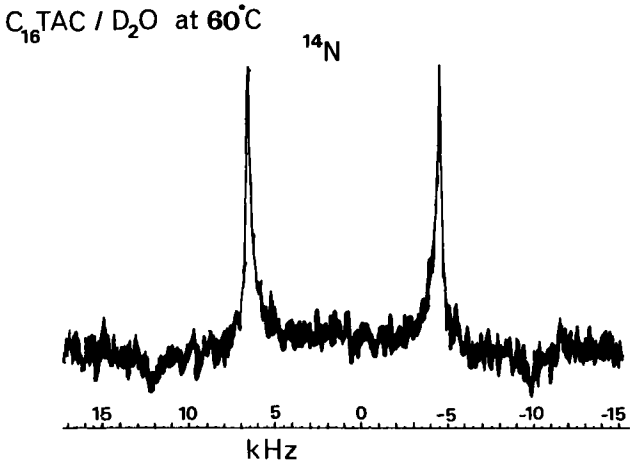

(*a*)

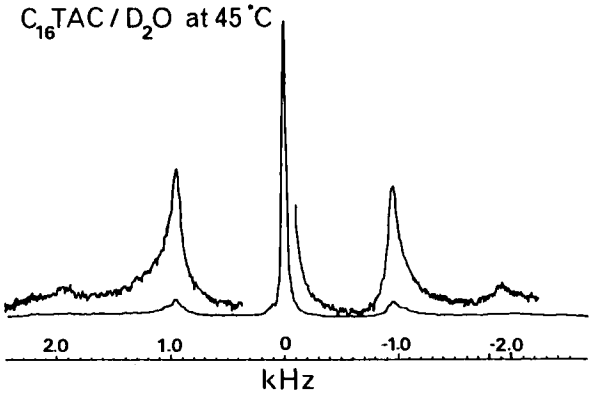

(*b*)

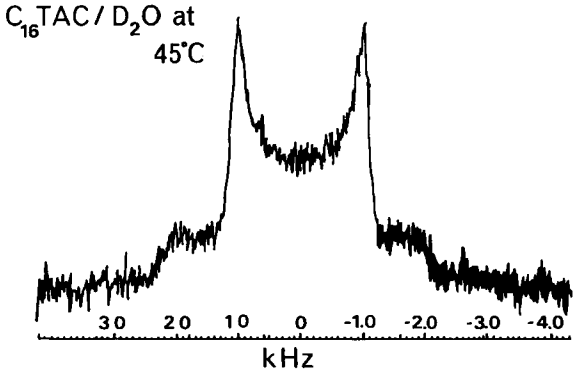

(*c*)

Figure 2. Typical NMR spectra for $C_{16}TAC$ samples (*a*) ^{14}N (H_1 phase); (*b*) ^{35}Cl (H_1 phase); (*c*) ^{2}H (L_α phase).

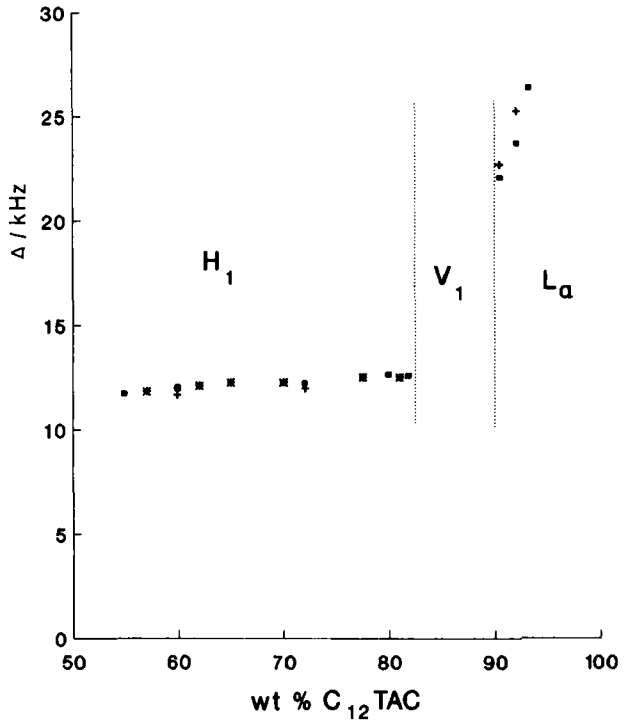

Figure 3. Nitrogen-14 quadrupole splitting values (Δ) for $C_{12}TAC/^2H_2O$ mixtures as a function of concentration. (■, 28°C; +, 45°C; ✱, 24°C).

the mesophases because the various different conformations resulting from different CH_2 positions for C_1–C_5 may result in different (averaged) values of χ. The uniaxial symmetry of the mesophases simplifies the treatment in that only the largest electric field gradient component (conventionally labelled V_{ZZ}) needs to be considered, but even then its alignment with respect to the molecular structure is not known. A fuller discussion is given in [23] and [26–29]. Molecular motion faster than the time scale of the NMR measurements reduces the value of χ. The motion results in a reduction of molecular order, described by the order parameter, S which reflects the degree of order of any given axis within the molecule. In the present case S describes the resultant ordering of the major electric field gradient component at the ^{14}N nucleus (V_{ZZ}). It is given by

$$S = \tfrac{3}{2}\langle \cos^2 \theta_{DM} \rangle - \tfrac{1}{2}, \tag{2}$$

where θ_{DM} is the angle between the liquid crystal uniaxis and V_{ZZ}, and the brackets $\langle\ \rangle$ represent a time average. As θ_{DM} varies from 0 to 90° then S may change from 1 through zero to $-1/2$. Due to the different orientation of the surfactant/water interface with respect to the uniaxis in the L_α and H_1 phases, and where *molecular* orientation and mobility are identical in both phases, we have

$$\Delta(L_\alpha) = -2\Delta(H_1). \tag{3}$$

(n.b. The sign of S cannot be obtained from the spectra reported here.)

Following this brief summary of the NMR theory, we see that the location and alignment of the $-NMe_3$ group is almost independent of composition for the H_1

phase because of the nearly constant Δ values (see figure 3). Whilst it is likely that the very small changes with surfactant concentration and temperature do arise from a variation in ordering, the exact nature of these (i.e., larger surface area per head group (*a*), altered conformational range of CH_2 groups, etc.) cannot be delineated without a better knowledge of V_{ZZ}. At the H_1/L_α boundary the increase in Δ is close to the expected factor of 2 (see equation (3)). Within the L_α phase, the water/surfactant molar ratio changes from 1·5 : 1 to 0·9 : 1 for the range of samples examined, while it is *c.* 3 : 1 for the H_1 samples at the H_1/V_1 boundary. Thus the solvent for the head groups in L_α consists of *c.* 50 per cent chloride ions. These occupy more space than water, hence an increase in Δ within this region may simply be a result of the change in solvent structure. Certainly, the *increase* in Δ with increasing temperature for L_α phase is unlikely to reflect a more ordered head group region.

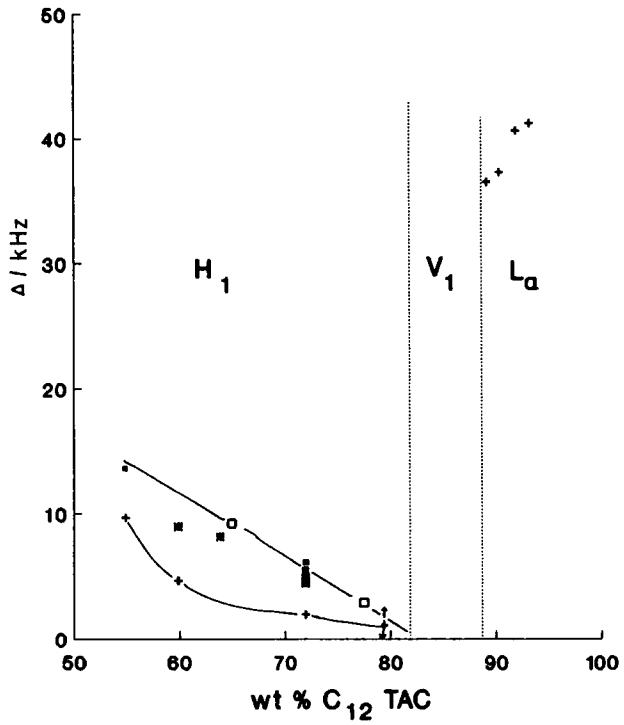

Figure 4. Chlorine-35 quadrupole splitting values (Δ) for $C_{12}TAC/^2H_2O$ mixtures as a function of concentration (■, 24°C; ✸, 25°C Bkr 322-S; +, 45°C; □, 24°C CXP 300).

In contrast to the ^{14}N data, figure 4 shows the sharp decrease of Δ (^{35}Cl) within the H_1 phase, and a decrease with increasing temperature. These observations confirm the earlier observations of Lindblom *et al.* [47], which also showed a decrease of Δ (^{35}Cl) with increasing concentration of $C_{12}TAC$ for the H_1 phase. The Δ value does approach zero prior to the transition to V_1; this was checked by examining the birefringence of the samples before and after the NMR measurement. Some difficulty was experienced in obtaining good spectra for the L_α phase because of the large Δ values, so measurements were made only at 45°C. (The total spectral width for ^{35}Cl ($I = 3/2$) is *c.* 4Δ.) Here Δ increased with concentration but to a smaller extent than the values for ^{14}N. Clearly, the change at the H_1/L_α boundary is considerably larger

than there expected factor of two. Because of their high symmetry, ions might be expected not to give quadrupole splittings since a zero electric field gradient should occur at the nucleus. However, non-zero gradients arise when the ion is close to a charged surface, or more importantly, from an asymmetric solvation shell at an interface [26]. Previously it has been demonstrated that only ions close to surfactant aggregates (< 3 Å) give a contribution to Δ values (termed bound ions), while those away from the surface have zero Δ values (free ions) [26, 30–32]. There is fast exchange between free and bound ions, hence the observed value is the weighted average

$$\Delta = p_f\Delta_f + p_b\Delta_b; \tag{4}$$

here the subscripts f and b refer to free and bound ions and Δ_f is assumed to be zero. Where several bound ion locations (sites) are possible then Δ is the average over all sites

$$\Delta = \sum_i p_{b,i}\Delta_{b,i}. \tag{5}$$

Because ion binding in mesophases roughly follows the ion-condensation hypothesis [32] we expect that Δ will be independent of composition where sufficient water is present to hydrate the ions fully. This is observed for sodium alkyl sulphates [32, 33]. For alkyl carboxylates, however, the ^{23}Na Δ values show behaviour resembling that observed above with the ^{35}Cl values for the H_1 phase [21, 30]. With increasing surfactant concentration there is a decrease of Δ to zero but this is followed by a monotonic increase again at very high concentration. It is now generally accepted that the change in Δ arises from a change in the angle between V_{ZZ} at the ion nucleus and the liquid crystal axis (θ_{DM}) [30]. At high water concentrations the sodium ions reside on the edge of the headgroup region, having V_{ZZ} perpendicular to the headgroup/water interface. As the water concentration is reduced then the ions replace water molecules between the headgroups, and the average angle between V_{ZZ} and the interface is reduced, so that $\langle\theta_{DM}\rangle$ decreases. As θ_{DM} passes through the so-called magic angle, Δ goes to zero and then increases again, having changed sign. The effect of increasing temperature is to move counterions from between headgroups to the edge of the region. Hence at high water concentrations Δ increases with temperature, while at low water levels it decreases to zero and then increases.

In the present case the ^{35}Cl Δ values resemble the behaviour of ^{23}Na values in decreasing with composition, but differ in that they *decrease* rather than increase with temperature. The latter implies that the ions reside between headgroups at the highest water concentrations, and are squeezed out as temperature or surfactant concentration is increased. This appears to be the most likely explanation at present, particularly because Δ for the L_α phase is larger than twice the highest H_1 value. However, further experiments are required to validate this tentative conclusion. The sensitivity of ^{35}Cl values to both composition and temperature is an indication of the absence of specific headgroup/counterion interactions since the average location of ^{35}Cl ions varies significantly with small changes of either one. Given the variation of Δ values within the H_1 phase it is unlikely that ^{35}Cl can be employed as a reliable structural probe without extensive work on model systems.

Water Δ values have been reported for a wide range of lyotropic systems. Where no exchangeable groups (e.g. OH, NH_2) are present in the surfactant then Δ arises from the ordering of surfactant-bound water molecules [27, 30]. These are in fast

exchange with free water having zero Δ. Thus Δ is given by

$$\Delta = \frac{3}{4}\sum_i p_{b,i} S_{b,i} \chi[^2H], \tag{6}$$

where $p_{b,i}$ is the fraction of water bound in site i with order parameter $S_{b,i}$ and $\chi(^2H)$ is the quadrupole coupling constant for the bound water. Following the definitive study of Halle and Wennerström, we take χ to be equal to the value for pure ^2H_2O (222 kHz) [27]. The order parameter $S_{b,i}$ refers to the average orientation of the O–^{2}H bond in the bound site. For water molecules interacting with surfactant headgroups via the H atoms then the non-interacting O–^{2}H bond directed away from the binding site is likely to have a very much smaller S_b value than that of the bound O–^{2}H bond. The fraction of bound water is dependent on the water/surfactant molar ratio (c). Where a large excess of free water is present p_b is expected to vary linearly with $1/c$, since the number of bound water molecules per surfacant (n_b) is constant. This is very commonly observed at low surfactant concentrations. At higher surfactant levels, where there is insufficient water to hydrate all the polar groups fully (typically $c < 10$) we intuitively expect Δ to increase sharply with concentration because $S_{b,i}$ increases and, perhaps χ (^{2}H) also increases. In practice, in this region for sodium dodecylsulphate [33], alkyl-polyoxyethylenes [34–36] and sodium laurate [21] Δ levels off and/or gives a maximum. A simple model which is consistent with this behaviour has been proposed [34–36], it considers the binding as a cooperative hydration shell governed by an equilibrium constant (K).

$$\text{Surfactant} + n_b\,(H_2O) \overset{k}{\rightleftharpoons} \text{surfactant}\,[H_2O]_{n_b}. \tag{7}$$

The reduction or levelling off of Δ arise from a reduced fraction of water present in the bound complex simply because the entropy of mixing eventually prevents all the water from becoming bound. From equation (7) it is a simple matter to show [36] that where S_b remains invariant, Δ first increases as a function of $1/c$, and passes through a maximum (as is observed experimentally [21, 33–36]) when $c = n_b - 1$. No measurements have been reported previously for the NMe_3^+ headgroup where water is not directly hydrogen bonded, but is bound by ion–dipole interactions. It is of considerable interest to see if the different binding interaction leads to the disappearance of the maximum.

The measured ^2H_2O Δ values are shown as a function of $1/c$ in figure 5. At low surfactant concentrations (in the H_1 phase) there is a linear increase of Δ with $1/c$ followed by a shallow maximum (see figure 5 (*a*)). This is followed by a sharp increase in the L_α phase. After allowing for the larger concentration of surfactant at the V_1/L_α boundary, this increase is much less than expected from equations (3) and (6), whether the initial linear portion or the high surfactant concentration region of the H_1 data is considered. The expanded figure of the H_1 data (see figure 5 (*a*)) shows some scatter of points between different batches of surfactant. This probably arises from the presence of small concentrations (~1 per cent) of alkylamines as impurities. The exchangeable N–^{2}H hydrogens will undergo fast exchange with ^2H_2O hydrogens. This has an effect on the measured Δ because the individual Δ values for N–^{2}H are large (several kHz), but the influence on the phase behaviour is very small. It contributes a systematic error to all the data for a given batch of material. Nevertheless, it is clear that the general pattern outlined here is valid, i.e. in the H_1 region Δ increases initially and then passes through a maximum. Also, there is a small increase in Δ with

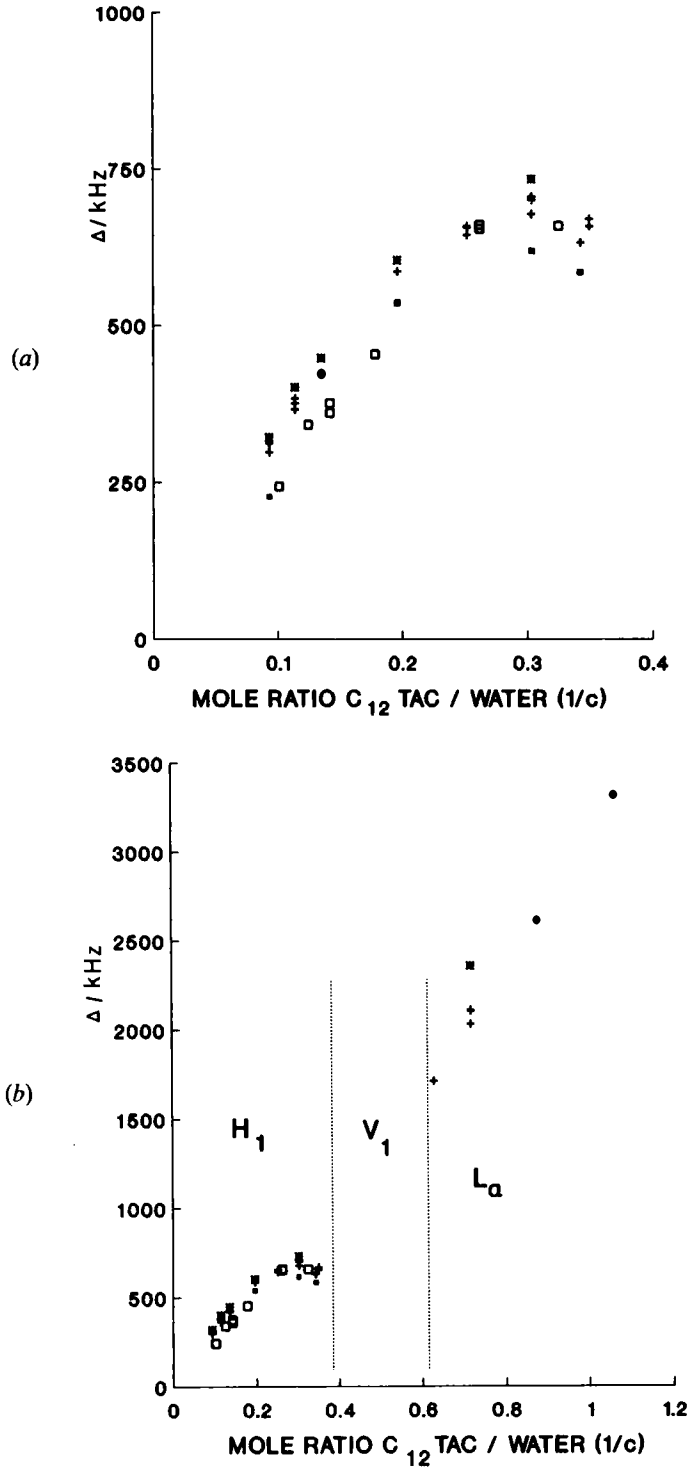

Figure 5. Deuterium quadrupole splitting values (Δ) for $C_{12}TAC/^2H_2O$ mixtures as a function of concentration (surfactant/water molar ratio, $1/c$). (*a*) Hexagonal phase; (*b*) Hexagonal and lamellar phases. (■, 24°C CXP-300; □, +, 25°C and 45°C. Bkr 322-S; ✸, 24°C, CXP-300, second batch of surfactant).

Table 1. The number of headgroup-bound water molecules (n_b) in H_1 and L_α phases derived from ^2H Δ values for various C_{12} surfactants.

Head Group	n_b (H_1)	n_b (L_α)	n_b (lct.) [37, 38]
$(-OCH_2CH_2-)_m$ OH [34]	2 m	1–1·5 m	2–5 m
$-SO_4Na$ [33]	10·6	< 4·6	8–9
$-CO_2Na$ [21]	10·1	< 5	8–9
$-NMe_3Cl$	4·3	< 2	5

increasing temperature. This is the opposite of what would be expected, since if anything, increasing temperature is expected to reduce p_b and S_b slightly due to the increased molecular motion of the headgroups and to increased entropy (favouring free water). The increase does indicate that the aligned O–^{2}H bond of the bound water is not along the normal to the surfactant/water interface, but at an angle to the normal. Hence changes in S arise from changes to this angle (θ_{DM}).

The observation that Δ (L_α) is less than 2Δ (H_1) means that considerable care must be exercised in using ^2H splittings as an indicator of mesophase structure, However, it does appear from figure 5 (*a*) that the simple theory [34–36] previously used to relate water binding and Δ values for nonionic surfactants can be used here. This allows an estimate of n_b (the number of headgroup-bound molecules) to be obtained. Table 1 lists the n_b values obtained from data in this and previous studies [21, 33, 34], assuming that the maximum in the Δ versus $1/c$ plot occurs when $c = n_b - 1$. The n_b values refer to fully hydrated headgroups. They also include water bound to counter-ions, since this does affect the concentration of free water, although it has a zero Δ value. The numbers shown in table 1 for the H_1 phase are in good agreement with other estimates made using self-diffusion and viscosity measurements [37, 38] on micellar solutions (right hand side column, table 1). The low value of n_b for the cationic surfactant is a consequence of the low hydration number for the counterion. A recent investigation of water binding to NMe_4^+ using self-diffusion coefficients of both ions and water [39] gave $n_b = 3{\cdot}6 \pm 1{\cdot}4$, again close to our estimate.

All of the studies in listed table 1 give Δ values for the L_α phase lower than expected; obviously when $c < n_b$, not all binding sites can be filled. Even so, it does seem that the number of binding sites is reduced in the L_α phase. This may simply be a geometric consequence of reduced micelle curvature and the smaller surface area per headgear (*a*) in L_α than in H_1. It is a factor that needs to be included in theoretical calculations of surfactant phase behaviour. We note that for the ionic surfactants in table 1 there is no sign of any maximum in the Δ values for the L_α phase. If we assume only modest changes in S_b, and that Δ (^2H_2O) is invariant, then we can place a limit on the value of n_b. Since S_b for the head-group bound O–^{2}H is *c.* 0·1–0·2 (from table 1 and equation (6)), while order parameters for the surfactant itself are often *c.* 0·2–0·4, S_b is unlikely to vary dramatically. Hence the limits in table 1 for n_b (L_α) are not unreasonable, given that they do *not* include counter-ion bound water. (The equilibrium at high surfactant concentrations is mainly between counter-ion bound water and head-group bound water.)

The NMR data show no qualitative differences between any of the mesophase systems in table 1. Thus for C_{12}TAC we find no evidence for any layers of structured water that could give rise to hydration forces despite the modern fashion for explaining unusual results with the concept. Similar conclusions were reported in a recent infra-red and far infra-red spectroscopic study of the water in this system [40]. In

addition this study gave evidence for the existence of two severely perturbed water species [40]. The significant differences observed between H_1 and L_α phase spectra resulted from *gradual* changes occurring in the V_1 phase. Unfortunately, it was not possible to investigate any correlation of the different bands with the concentration of different bound water species because of low absorption band intensities.

3.2. *Hexadecyltrimethylammonium chloride ($C_{16}TAC$)/water system*

The phase diagram for this system is shown in figure 6. It is based on the collected results of optical microscopy, DSC, NMR and X-ray diffraction. Above 40°C, H_1 and L_α phases occur; they are separated by V_1 or *Int.* phases according to the method of preparation and temperature. The behaviour of this region is complex, and forms the subject of a further report in this series [18]. On heating, optical microscope penetration scans of $C_{16}TAC$ with water clearly show *Int.* phases between H_1 and L_α from *c.* 37–67°C with V_1 appearing in the middle of the *Int.* region at *c.* 55°C (see plate 2 and table 1, [5]). On cooling the V_1 supercools below 35°C very readily and the *Int.* region does not reappear. Below *c.* 40°C at equilibrium the more concentrated surfactant mixtures form an interdigited gel phase (see later and figure 7) which is separated by a fairly large two-phase region from H_1. Solid surfactant in equilibrium with the gel phase or L_α occurs at very high surfactant compositions. This part of the diagram was not investigated in detail, hence the boundary is very uncertain.

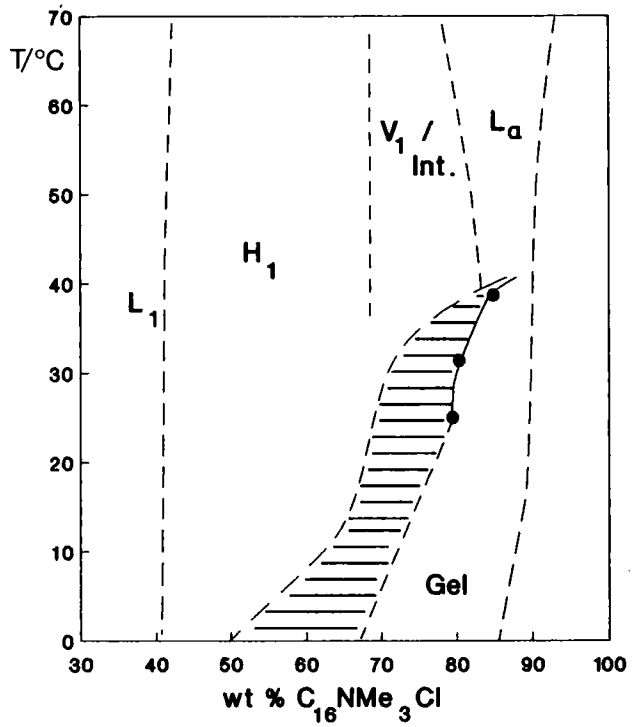

Figure 6. Partial phase diagram of hexadecyltrimethylammonium chloride ($C_{16}TAC$)/^2H_2O system. Phase boundaries are dotted to indicate that no attempt was made to locate them to an accuracy of better than 2 per cent. H_1, hexagonal phase; L_α lamellar phase; gel, interdigited monolayer phase (see text); *Int.*/V_1 region, phase structure varies according to temperature cycle, see [18].

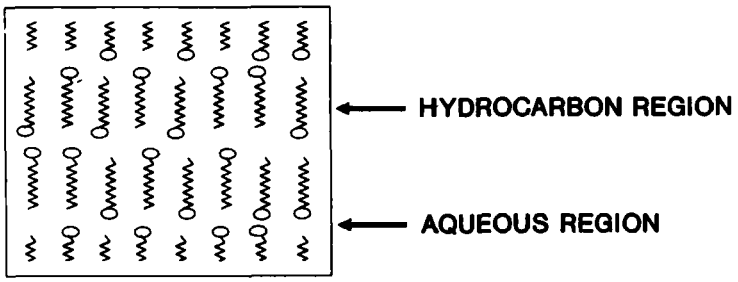

Figure 7. Schematic representation of the interdigited gel phase structure.

3.2.1. *Optical microscopy and DSC measurements*

The only fairly novel phase in figure 6 that is described here is the gel (*Int.* phases will be described in a future report [18]). It can be recognized because it is very, very viscous, (it hardly moves at all when the cover-slip is pressed) and has distinct textures which, however, bear some resemblance to those of L_α (see figure 8). Many of the gross features of the L_α texture are retained in the gel, but note the much finer texture present in the micrograph of the gel phase. Where homeotropic regions occur with L_α, they are often preserved to some extent on rapid (< 10 s) cooling into the gel phase. (Rapid cooling ensures that the composition heterogeneity arising from the two-phase region is small.) Since the gel phase layers are thinner than those in L_α (see later), the molecular mechanism which preserves the uniaxis alignment would seem to involve the dissociation of some bilayers and formation of monolayers between existing bilayers. A study of the kinetics of this process could provide much interesting information on the fundamental mechanisms of self-aggregation and order in these systems.

The DSC of the anhydrous surfactant is reported to show a single transition at 95°C with ΔH of 41·8 kJ mol^{-1} which reappears on cooling [25]. Below 50 per cent surfactant in water the behaviour is similar to that of C_{12}TAC. There are no major transitions not associated with the dissolution of solid surfactant or gel in melted ice. Above this concentration the gel/mesophase peak appears initially as a fairly broad transition, but becoming narrower at high concentrations as the two-phase region narrows (see figure 6). Because of the large transition width, the measured ΔH values were somewhat variable, falling in the range 18–24 kJ mol^{-1} (of C_{16}TAC). There was no obvious change with surfactant concentration, or which mesophase was formed above the gel. The magnitude of ΔH is only slightly smaller than the range of values reported for the gel phase melting of trioxyethyleneglycolhexadecylether ($C_{16}EO_3$, 26–32 kJ mol^{-1}) [41]. For $C_{16}EO_3$ the gel phase also melts at *c.* 40°C, but the melting temperature is almost independent of water content, unlike the C_{16}TAC behaviour. In the present case it is likely that the increased counter-ion dissociation and head-group hydration in the H_1 and L_1 phases are important contributions to this difference. This similarity between the gel/mesophase transition entropies and the large transition entropy for anhydrous C_{16}TAC strongly supports the conclusion of Iwamoto *et al.* [25] that the latter exists as a mesophase rather than a solid above 95°C. A gel $\rightarrow$ L_1/mesophase transition similar to that reported in figure 6 has been observed for octadecyltrimethylammonium chloride (C_{18}TAC) by Kodama and co-workers [42–4]. Their measured transition entropy is in excellent agreement with the data reported here. These authors give no details of the phase structure above the gel melting transition.

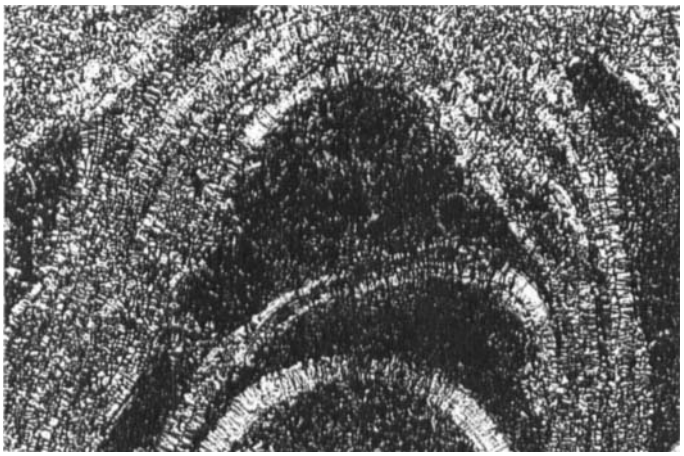

(*a*)

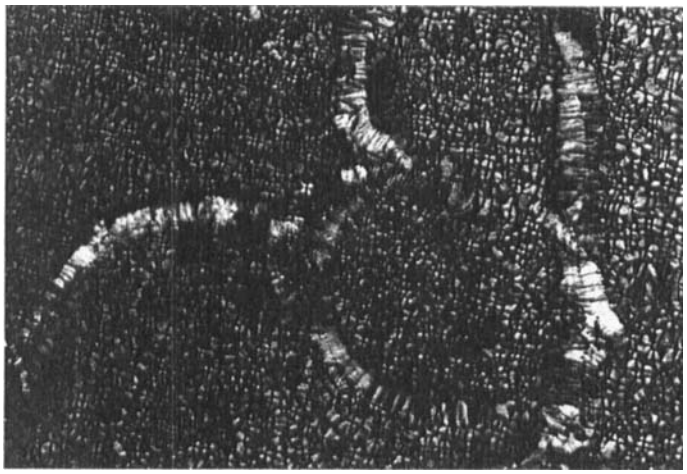

(*b*)

Figure 8. Optical micrographs of (*a*) gel phase, 25°C; (*b*) L_α phase 45°C (85 per cent C_{16}TAC, crossed polars, *c.* × 200).

3.2.2. *Low-angle X-ray diffraction studies*

The only data on this system reported here are for the gel phase at 25°C. Data on the various other liquid crystal phases are to be included in the next report [18]. At 25°C the gel phase is limited to > 77 per cent C_{16}TAC concentration. Nevertheless, the few measurements made (see table 2) give conclusive proof of the interdigited monolayer structure. Sharp diffraction lines in the ratios $d_0 : d_0/2$ were obtained for all samples. If the densities of surfactant and water layers are known it is a simple matter to calculate the hydrocarbon and aqueous region thicknesses [19]. From the density of hexadecyltrimethylammonium bromide (C_{16}TAB) in the gel phase reported by Vincent and Skoulios [45] we calculate that of C_{16}TAC to be 1·013 g cm^{-3} after allowing for the smaller ionic radius of Cl^- (1·81 Å) compared to BR (1·96 Å). This gives [1] the surfactant layer thickness of 27·8 ± 0·2 Å, including headgroups and

Table 2. X-ray data (25°C) for gel phase of $C_{16}TAC/^2H_2O$ samples. (d_0 = layer separation; d_a, d_w = surfactant layer, water layer thickness; d_a includes headgroups—see text).

Percentage $C_{16}TAC$	d_0/Å	d_a/Å	d_w/Å	a/Å^2
81·8	33·3	27·7	5·6	37·9
83·9	32·6	27·7	4·9	37·8
	32·9	28·0	4·9	37·5

Density of $C_{16}TAC$ = 1·013 g cm^{-3}; density ^2H_2O = 1·11 g cm^{-3}.

counterions. The headgroup extends ~4 Å from the 1-CH_2 group of the C_{16} chain; hence the C_{16} chain extension estimated from the data is 19·8 Å. This compares very well with a value of 20 Å calculated for an all-trans C_{16} chain from known bond lengths, giving the best evidence for the structure shown in figure 7. Thus the aqueous region is *c.* 13 Å thick including headgroups and counterions, rather than the value of 5 Å given in table 2. Also consistent with the structure given in figure 7 is the value of a, which is close to that expected for two all-trans chains. Vincent and Skoulios reported data on the $C_{16}TAB$ gel phase along with data on soap gel phases over 20 years ago [45], but this had attracted almost no attention since then. Our measurements on the $C_{16}TAC$ gel structure are in excellent accord with their results.

3.2.3. *NMR measurements*

Here we describe NMR measurements on the H_1, L_α and gel phases only. The data for the $V_1/Int.$ region are complex and are reserved for the subsequent paper [18]. Typical NMR spectra are given in figure 2 and quadrupole splittings of the various nuclei (^{14}N, ^{35}Cl and ^2H) at 45°C for H_1 and L_α phases are shown in figures 9–11. It proved to be impossible to measure ^{14}N and ^{35}Cl Δ values for the gel phase, despite the easy detection of the $-1/2 \rightarrow +1/2$ transition for ^{35}Cl and prolonged signal averaging in both cases. The reason for this is likely to be the occurrence of very large Δ values (outside the range of the spectrometer) due to the reduced motional averaging of electric field gradients.

For the H_1 phase ^{14}N Δ values of $C_{16}TAC$ (see figure 9) are almost identical to those for $C_{12}TAC$ at the same temperature. The L_α values are in the same range, but are slightly larger for $C_{16}TAC$. Comparison of figures 10 and 4 shows broadly similar behaviour of the ^{35}Cl Δ values in both cases, but the $C_{16}TAC$ values are generally larger than those of C_{12} whether compared on a weight fraction or a mole ratio scale. Our ^{35}Cl Δ values at 45°C are slightly smaller than the single value previously reported for 55 per cent $C_{16}TAC$ at 28°C (18·5 kHz) [46], as expected from the temperature dependence of Δ for $C_{12}TAC$. Also we observed Δ to be 4·3 kHz larger at 20°C than at 45°C for 60 per cent $C_{16}TAC$, in excellent agreement with the previous report [46]. Note that repeated measurement of ^{14}N Δ values on the same sample over a period of several years gave values in agreement to better than 1 per cent. Hence the scatter shown on figure 10 probably arises from differences in the probe temperature, rather than inaccuracies in measuring the spectra.

The largest difference between the Δ values for the two surfactants occurs with the measurements on ^2H_2O. With $C_{16}TAC$ the Δ values are much lower. Because of the small values it was possible to resolve Δ for only two H_1 samples. The lower surfactant concentration samples did show line broadening, so the half height width ($\Delta V_{1/2}$) of

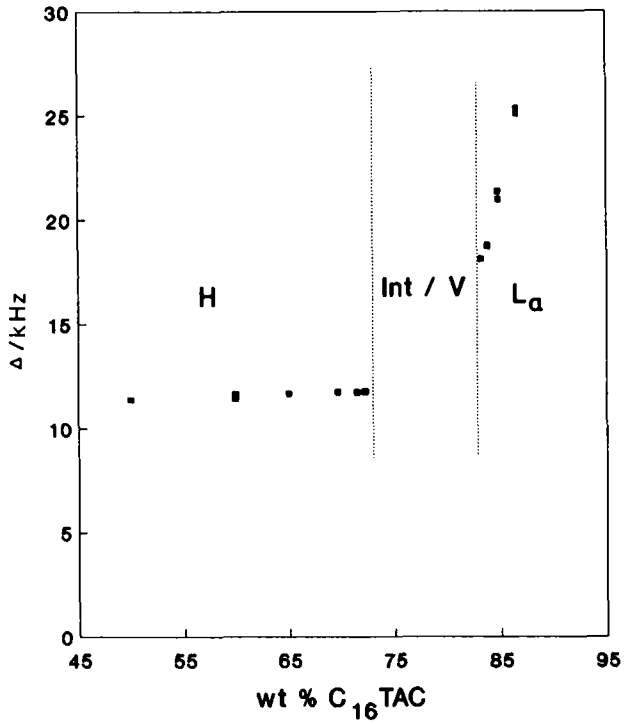

Figure 9. Nitrogen-14 quadrupole splitting values (Δ) for $C_{16}TAC/^2H_2O$ mixtures as a function of concentration at 45°C.

the spectra is shown in figure 11. At the H_1/L_α transition, after allowing for the increased concentration in L_α, Δ (^2H) changes by a factor of 2. This indicates that no change in n_b occurs at this point. Since $1/c = 0{\cdot}2$–$0{\cdot}3$ this is the region where Δ still increases with $1/c$, and so we cannot be certain that n_b is smaller for $C_{16}TAC$ than for $C_{12}TAC$. Beyond this (in L_α) Δ increases sharply and then levels off (one sample only). The increase probably arises from a change in S (see later), while with the final sample we suspect the presence of crystalline $C_{16}TAC$, hence the composition of the phase is $1/c < 0{\cdot}5$ (see later).

The Δ values for the H_1 phase in $C_{16}TAC$ are reduced by 50 per cent compared to the value for $C_{12}TAC$. This is unexpected, and probably arises becasue θ_{DM} is close to the magic angle, hence changes in micelle curvature (C_{12}–C_{16}) exert an exceptional influence. For other systems no chain length dependence of Δ is observed. This sensitivity probably accounts for the steep increase in Δ over the range $1/c = 0{\cdot}35$–$0{\cdot}4$ and for the temperature sensitivity of the data. (This is the same explanation that was proposed to account for the temperature dependence of Δ for $C_{12}TAC$.) We cannot be certain that the levelling off of the curve at very high concentration is valid, since the gel phase Δ value at 40°C for this sample is similar to that of lower sample, hence some solid could be present.

Figure 12 illustrates Δ values for the gel phase at two temperatures. The Δ versus $1/c$ curve appears linear up to $1/c \approx 0{\cdot}3$, and then became steeper. Note that Δ values at 25°C are larger than those at 5°C; this trend is continued at least to 40°C. The strong (for ^2H_2O) temperature dependence suggests that, as for the L_α phase, the bound O–^2H bond is not normal to the surfactant/water surface, hence S is probably changing in the range $1/c > 0{\cdot}3$. This invalidates any attempt to use

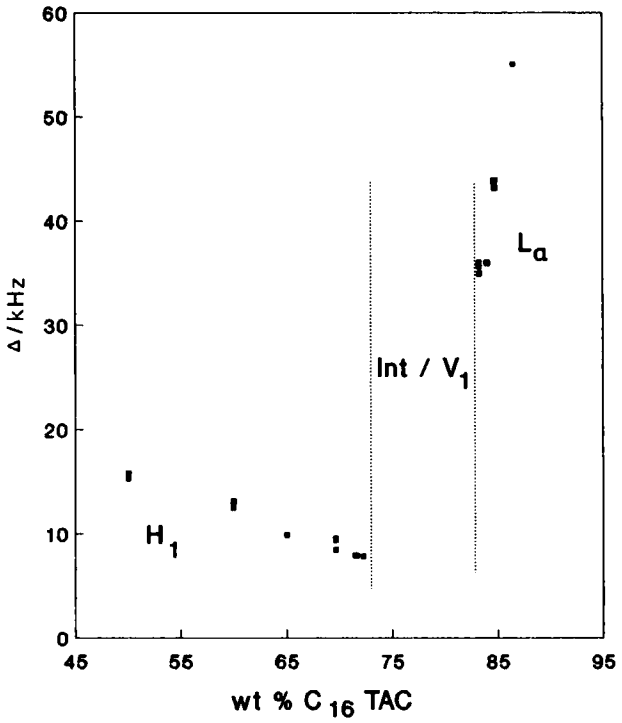

Figure 10. Chlorine-35 quadrupole splitting values (Δ) for $C_{16}TAC/^2H_2O$ mixtures as a function of concentration at 45°C.

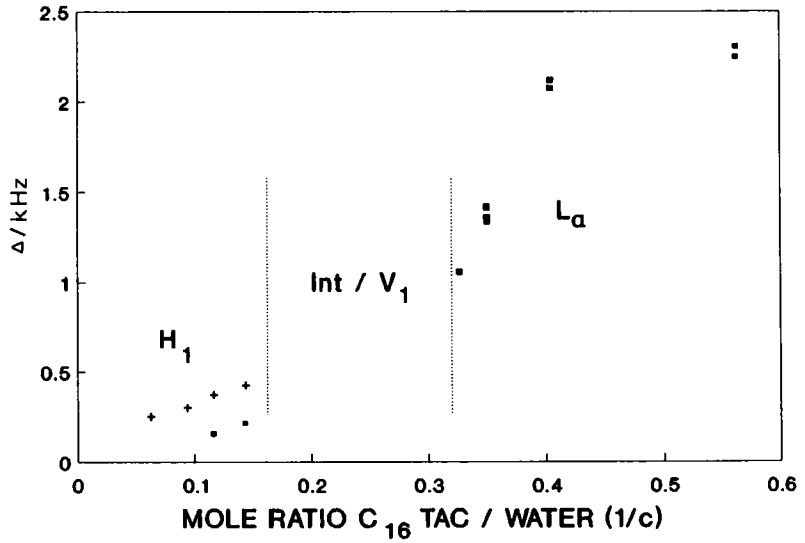

Figure 11. Deuterium quadrupole splitting values (Δ) and half-height width ($\Delta V_{1/2}$) for $C_{16}TAC/^2H_2O$ mixtures as a function of concentration at 45°C, (■, Δ; + $\Delta V_{1/2}$).

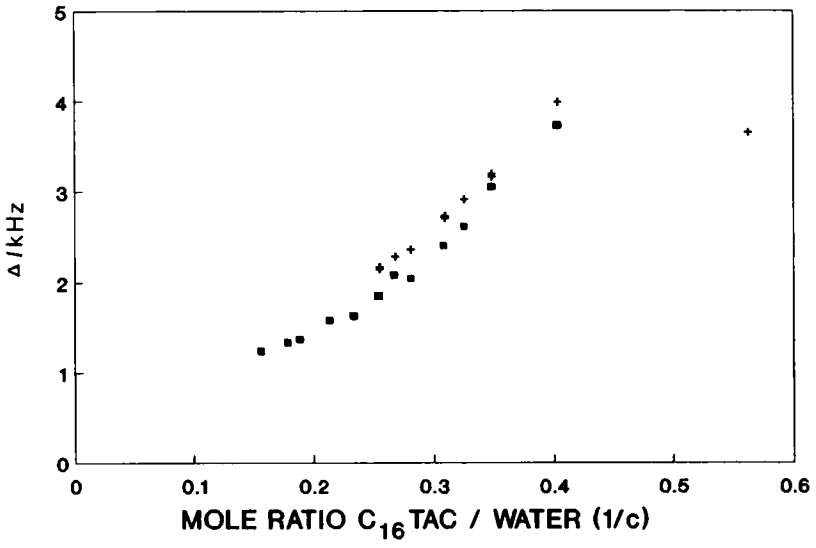

Figure 12. Deuterium quadrupole splitting values (Δ) for $C_{16}TAC/^2H_2O$ samples in the gel phase as a function of surfactant/water mole ratio, (■, 5°C; +, 25°C).

^2H Δ values to obtain n_b values, except to say that $n_b < 4$, which is hardly a startling conclusion.

Finally, in this section we report the proton alkyl chain T_{2eff} value for the gel phase at 24°C as 30·5 ± 1 μs, independent of composition. T_{2eff} is the time taken for the proton free induction decay following a $\pi/2$ pulse to be reduced to 1/e of the initial intensity [41]. The value of T_{2eff} is characteristic of a particular phase structure (see, e.g., [21]) reflecting the degree of ordering of the alkyl chain. The measurements were made as described in [41]. This value is the same as that reported [41] for the C_{16} chains in $C_{16}EO_3$ gel phase (30 μs) providing further evidence for the 'interdigited-monolayer' structure.

4. General comments

In this paper we have demonstrated that ^{14}N and ^{35}Cl spectra are easy to obtain for cationic surfactant liquid crystals hence the Δ values can be measured. The ^2H spectra can also give Δ values, particularly for gel and L_α phases. These techniques will clearly be invaluable for studies of molecular interactions and ordering. For mesophase structure studies it seem that ^{14}N NMR will be the best technqiue. The Δ values listed here obtained on well-defined systems can be used to evaluate phase structures of novel surfactants, provided that a large enough range of compositions is examined.

The agreement between n_b values derived from ^2H NMR measurements with those obtained by other methods provides gratifying support for the theory relating hydrogen-bonded water to hydration forces [36]. Also, the sensitivity of the ^{25}Cl Δ values to temperature and composition indicates that measurement of ^{35}Cl Δ values could be employed to monitor the interaction of ^{35}Cl ions with the headgroup/water interface whenever specific adsorption or desorption is suspected (including polymer mesophase systems). We shall demonstrate the utility and limitations of these

techniques for structural investigations in a subsequent paper [18], which will describe what happens in the range 78–82 per cent C_{16}TAC.

References

[1] LUZZATI, V., 1968, *Biological Membranes*, Vol. I, edited by D. Chapman (Academic Press), p. 71.
[2] WINSOR, P. A., 1968, *Chem. Rev.*, **68**, 1.
[3] EKWALL, P., 1971, *Advances in Liquid Crystals*, Vol. I, edited by G. H. Brown (Academic Press), p. 1.
[4] TIDDY, G. J. T., 1980, *Phys. Rep.*, **57**, 1.
[5] BLACKMORE, E. S., and TIDDY, G. J. T., 1988, *J. chem. Soc. Faraday, Trans II*, 2 **84**, 1115.
[6] HALL, C., and TIDDY, G. J. T., 1986, *Proceedings of the Sixth International Symposium on Surfactants in Solution*, edited by K. L. Mittal; 1989, *Surfactants in Solution*, Vol. 8, p. 9.
[7] TIDDY, G. J. T., 1986 (unpublished results).
[8] KEKICHEFF, P., and TIDDY, G. J. T., 1989, *J. phys. Chem.*, **93**, 2520.
[9] KEKICHEFF, P., CABANE, B., and RAWISO, M., 1986, *J. Phys. Lett., Paris*, **45**, L813.
[10] KEKICHEFF, P., and CABANE, B., 1987, *J. Phys., Paris*, **48**, 1571.
[11] WOOD, R. M., and MCDONALD, M. P., 1985, *J. chem. Soc. Faraday Trans. I*, **81**, 273.
[12] CHIDICHIMO, G., GOLEMME, A., and DOANE, J. W., 1985, *J. chem. Phys.*, **82**, 4369.
[13] TIDDY, G. J. T., 1985, *Modern Trends of Colloid Science in Chemistry and Biology*, edited by H. F. Eicke (Birkhauser Verlag), p. 148.
[14] KEKICHEFF, P., and CABANE, B., 1988, *Acta crystallogr.* B, **44**, 395.
[15] LUZZATI, V., TARDIEU, A., and GULIK-KRZYWICKI, T., 1968, *Nature, Lond.*, **217**, 1028.
[16] HOLMES, M. C., and CHARVOLIN, J., 1984, *J. phys. Chem.*, **88** 810.
[17] SCHOEN, A. H., 1970, *NASA Tech. Note D55421* (Natn. Tech. Inf. Serv., Springfield), Document N70-29782.
[18] BLACKMORE, E. S., and TIDDY, G. J. T. (in preparation).
[19] BROOME, F. K., HOERR, C. W., and HARWOOD, H. J., 1951, *J. Am. chem. Soc.*, **73**, 3350.
[20] BALMBRA, R. R., CLUNIE, J. S., and GOODMAN, J. F., 1969, *Nature, Lond.*, **22**, 1159.
[21] RENDALL, K., TIDDY, G. J. T., and TREVETHAN, M. A., 1983, *J. chem. Soc. Faraday Trans. I*, **79**, 637.
[22] FOX, K., FONTELL, K., and HANSSON, E., 1985, *Molec. Crystals liq. Crystals, Lett.* p. 9. ERIKSSON, P. O., LINDBLOM, G., and ARVIDSON, G., 1985, *J. phys. Chem.*, **89**, 1050.
[23] SODERMAN, O., WALDERHAUG, H., HENRIKSSON, U., and STILBS, P., 1985, *J. phys. Chem.*, **89**, 3693.
[24] ROSEVEAR, F. B., 1954, *J. Am. Oil chem. Soc.*, **31**, 628.
[25] IWAMOTO, K., OHNUKI, Y., SAWADA, K., and SENO, M., 1981, *Molec. Crystals liq. Crystals*, **73**, 95.
[26] WENNERSTROM, H., LINDBLOM, G., and LINDMAN, B., 1974, *Chem. scripta.*, **6**, 97.
[27] HALLE, B., and WENNERSTROM, H., 1981, *J. chem. Phys.*, **75**, 1928.
[28] ERIKSSON, P. O., KHAN, A., and LINDBLOM, G., 1982, *J. phys. Chem.*, **86**, 387.
[29] PRATUM, T. K., and KLEIN, M. P., 1983, *J. magn. Reson.*, **53**, 473.
[30] LINDBLOM, G., LINDMAN, B., and TIDDY, G. J. T., 1978, *J. Am. chem. Soc.*, **100**, 2299.
[31] TIDDY, G. J. T., LINDBLOM, G., and LINDMAN, B., 1978, *J. chem. Soc. Faraday Trans. I*, **74**, 1290.
[32] WENNERSTROM, H., LINDMAN, B., LINDBLOM, G., and TIDDY, G. J. T., 1979, *J. chem. Soc. Faraday Trans. I*, **75**, 663.
[33] LEIGH, I. D., MCDONALD, M. P., WOOD, R. M., TIDDY, G. J. T., and TREVETHAN, M. A., 1981, *J. chem. Soc. Faraday Trans. I*, **77**, 2867.
[34] RENDALL, K., and TIDDY, G. J. T., 1984, *J. chem. Soc. Faraday Trans. I*, **80**, 3339.
[35] LYLE, I. G., and TIDDY, G. J. T., 1986, *Chem. Phys. Lett.*, **124**, 432.
[36] CARVELL, M., HALL, D. G., LYLE, I. G., and TIDDY, G. J. T., 1986, *Faraday Discuss. chem. Soc.*, **81**, 223.
[37] WENNERSTROM, H., and LINDMAN, B., 1979, *Phys. Rep.*, **52**, 1.
[38] LINDMAN, B., and WENNERSTROM, H., 1980, *Topics in Current Chemistry*, **87**, 1.
[39] ERIKSSON, P. O., LINDBLOM, G., BURNELL, E. E., and TIDDY, G. J. T., 1988, *J. chem. Soc. Faraday Trans. I*, **84**, 3129.

[40] PACYNKO, W. F., YARWOOD, J., and TIDDY, G. J. T., 1987, *Liq. Crystals*, **2**, 201.
[41] ADAM, C. D., DURRANT, J. A. LOWRY, M. R., and TIDDY, G. J. T., 1984, *J. chem. Soc. Faraday Trans. I.*, **80**, 789.
[42] KODAMA, M., KUWABARA, M., and SEKI, S., 1982, *Thermal. Anal., Proc. Int. Conf. 7th*, p. 822.
[43] KODAMA, M., and SEKI, D., 1983, *Prog. colloid Polym. Sci.*, **68**, 158.
[44] KODAMA, M., and SEKI, S., 1984, *Hyomen*, **22**, 61.
[45] VINCENT, J. M., and SKOULIOS, A., 1966, *Acta crystallogr.*, **20**, 441.
[46] FABRE, H., KAMENKA, N., KHAN, A.,, LINDBLOM, G., LINDMAN, B., and TIDDY, G. J. T., 1980, *J. phys. Chem.*, **84**, 3428.
[47] LINDBLOM, G., PERSSON, N. O., and LINDMAN, B., 1973, *Chemie, Physikalische Chemie und Anwendungstechnik der grenzflachenaktiven Stoffe*, Vol. II (Carl Hanser Verlag), p. 939.